RESIN FLOW IN COMPRESSION MOLDING PROCESSES

P. Bockelmann[1], J. Maierhofer[1], J. Krollmann[1], S. Zaremba[1], K. Drechsler[1], P. Mertiny[2]

[1]Institute for Carbon Composites, Faculty of Mechanical Engineering, Technische Universität München, Boltzmannstrae 15, D-85748 Garching b. München, Germany
Email: bockelmann@lcc.mw.tum.de, Web Page: http://www.lcc.mw.tum.de
Email: j.maierhofer@tum.de, krollmann@lcc.mw.tum.de, zaremba@lcc.mw.tum.de, drechsler@lcc.mw.tum.de
[2]Advanced Composite Materials Engineering Group, Faculty for Mechanical Engineering, University of Alberta, Edmonton, Canada, Email: pmertiny@ualberta.ca, Web Page: http://www.mece.ualberta.ca

Keywords: Wet compression molding, Carrier-integrated pressing, Fiber-reinforced plastics, Matrix flow, Fluorescent photography

Abstract
Wet compression molding (WCM) of continuous fiber-reinforced composites is an alternative to resin transfer molding (RTM) to produce parts of low-complexity and small dimensions in high volumes. We hypothesize that matrix flow in WCM is chaotic due to matrix pre-application onto the fiber materials. An alternative process, carrier-integrated pressing (CIP) could solve this conflict by a spacial separation of matrix and fiber material with storage of the matrix inside cavities of a carrier.

Matrix flow in plates produced by WCM and CIP was studied with a newly developed evaluation method that allows to trace the distribution of matrix with fluorescent photography. Experiments conducted within design of experiments (DoE) studies lend evidence to the hypothesis of matrix pre-application, matrix flow control and material stabilization. It was found that the flow of fluorescent matrix was highly heterogeneous in WCM with low initial flow in through-thickness direction. Matrix distribution was much more compact with good control of the flow in CIP via relapse of cavities under process heat.

1. Introduction and Research Questions

There is agreement that controlled homogeneous resin flow in liquid composite molding (LCM) processes promotes low porosity, absence of dry spots and robust processing of composites, e. g. [1]. Current high volume production processes are based on the two LCM variants resin transfer molding (RTM) and wet compression molding (WCM) [2]. While impregnation mechanisms in RTM have been studied intensively, there is little understanding of resin flow in WCM processes.

WCM is a relatively inexpensive process based on pre-applicating liquid matrix superficially on planar continuous dry fiber material. The wet stack is then shaped, compacted and cured during one press stroke [3, p. 14]. Superimposing drape and impregnation impacts production in two ways. Firstly, it helps to reduce mold occupancy time and number of coupled processes [4, p. 43]. Secondly, the resin flow impregnates fibers mainly in through-thickness direction. Therefore, resin can still permeate dense fiber materials [3, p. 14] and curing time can be reduced compared to RTM.

Due to a low permeability of rovings perpendicular to their longitudinal direction [5, p. 104] it is expected

Excerpt from ISBN 978-3-00-053387-7

that the bulk of matrix forms a film on top of the NCF stack. A liquid matrix film is prone to dislocation due to inertia during transport of the material into the press . Furthermore, without any stabilization, matrix flow during compression is subject to an inhomogeneous initial position and may become highly heterogeneous in nature due to a heterogeneous permeability distribution, Figure 1.

Carrier-integrated pressing (CIP) has been proposed as an alternative process to improve resin flow control [6] [7]. CIP is based on a spacial separation of matrix and fiber material with the matrix being stored in carrier cavities in proximity of its final curing location. The carrier allows controlled storage of matrix in relation to the fiber material subsequent to pre-application. The release of matrix from storage cavities is initiated when cavities are deformed. Pre-application of matrix is not disturbed by the stabilization of materials and preparation can be performed outside of press. Due to the defined storage of matrix close to its subsequent curing location, it can be hypothesized that matrix flow is of higher homogeneity compared to WCM, Figure 1.

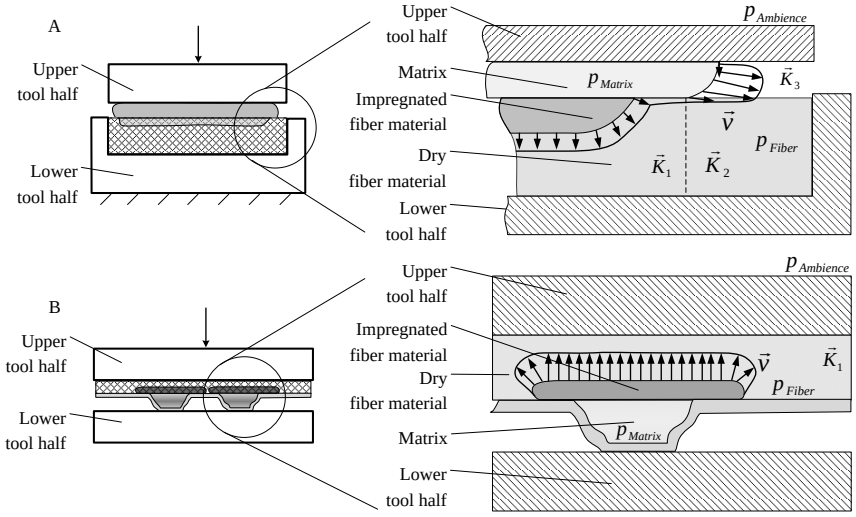

Figure 1. Hypothetical flow situations in WCM (A) and CIP (B)

No information on matrix flow in WCM processes have been published so far and the conflict between pre-applicated matrix and controlled matrix flow during pressing hypothesized in Figure 1 has not been tested. In particular, it is not known, how the process parameters of each process influence matrix flow during compression. Thus, the following research question shall be investigated in this paper:

How does matrix flow through fiber material in WCM and CIP?

During pressing, the carrier cavities in CIP are eliminated. This elimination influences matrix position before and its flow during pressing and leads to the connected question of:

How is cavity elimination linked to matrix flow?

In the following sections, the investigation of both questions is presented. Firstly, the method, fluorescent photography, which is used to quantify the flow is described. Subsequently, a Design of Experiment (DoE) study for each process, WCM and CIP, to vary the process parameters is detailed. The results of this study are then presented and interpreted in regard to the formulated research questions.

Excerpt from ISBN 978-3-00-053387-7

2. Materials and Methods

2.1. Tracing Matrix Flow by Fluorescent Photography

In order to study matrix flow in compression molding processes, we propose to detect the spatial distribution of individual matrix accumulations via fluorescence markers. The flow is interpreted by computer-aided segmentation of digital images of the final distribution of marked matrix. Quantifying criteria are proposed in regard to the compactness of the flow, since a compact matrix distribution after pressing is associated with good flow control and vice versa. The compactness is expressed by criteria of distribution of the marked matrix and secondly, its path between initial and final location explained in Figure 2.

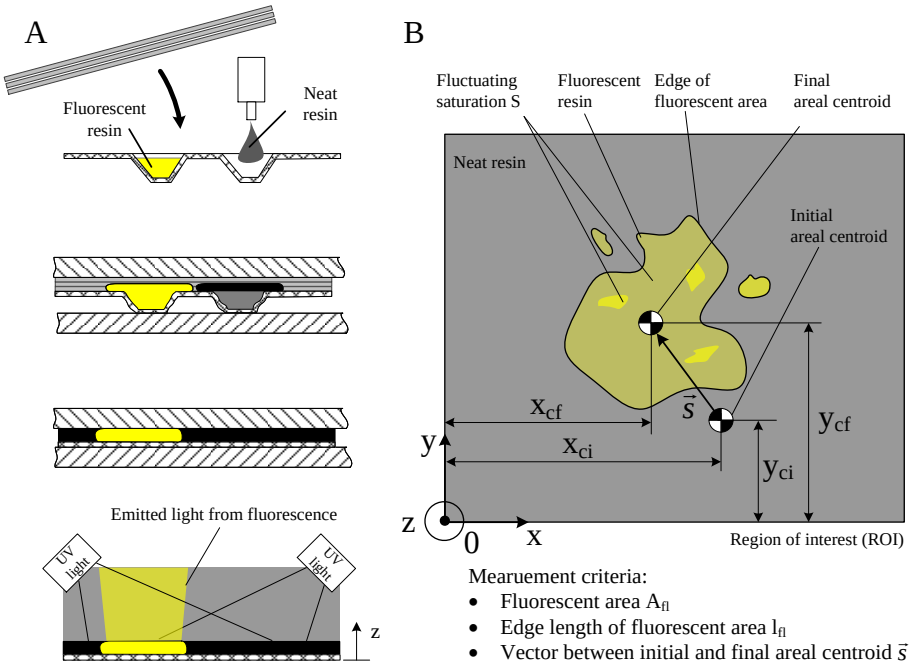

Figure 2. Processing principle (A) and criteria to quantify matrix flow regarding distribution and flow path of fluorescent resin (B). Resin distribution is described by fluorescent area A_{fl} and its edge length l_{fl}, vector $\vec{s}$ represents the flow path between initial and final areal centroids. Most compact distribution is reached when criteria are minimized

The criteria derived in Figure 2 to describe compactness and flow of fluorescent matrix are converted to quality parameters Q_1 (ratio of fluorescent area), Q_2 (ratio of edge length) and Q_3 (shift of areal centroid), which are set in relation to the respective criteria in reference to the entire region of interest (ROI):

$$Q_1 = \frac{A_{fl}}{A_{roi}} \tag{1}$$

with $Q_1 \in [0; 1]$, fluorescent area A_{fl} and area of ROI A_{roi}.

$$Q_2 = \frac{l_{fl}}{l_{roi}} \tag{2}$$

with $Q_2 \in [0; \infty]$, l_{fl} beeing the edge length of A_{fl} and l_{roi} the edge length of A_{roi}.

Parameter Q_3 quantifies the absolute value of the position vectors for initial and final areal centroids:

Excerpt from ISBN 978-3-00-053387-7

$$Q_3 = mean(|\vec{s}_i|) = mean(|\vec{s}_{cf} - \vec{s}_{ci}|) = \sqrt{(x_{cf} - x_{ci})^2 + (y_{cf} - y_{ci})^2} \quad (3)$$

with $Q_3 \in \mathcal{R}$, position vector of initial areal centroid $\vec{s}_{ci}$ and position vector of final areal centroid $\vec{s}_{cf}$.

With the parameters above, a compact matrix distribution is reached with a minimal Q_1, Q_2 and Q_3.

The derived quality parameters are computed from digital images, following the construct of computerized image processing, discussed elsewhere [8, p. 13]. Images are acquired by digital single lens reflex camera Canon EOS 7D with a 17-40 L USM lens. Photographs are taken at a focal distance of 40 mm with an f13.0 aperture and 10 s exposure time. The white balance is set to sunshine and the Iso-photosensitivity remains at 100. The camera is mounted on a tripod and adjusted vertically above the part to be photographed. The part is positioned within an alignment rig, which carries four identical UV lamps (LF-106S from Uvitec). The lamps emit light of a wavelength of 254 nm. The images are processed drawing on algorithms from the Image Processing Toolbox in Matlab to compute the quality parameters defined in Equations 1-3 based on the color model Hue-Saturation-Value (HSV) [8]. The algorithm recognizes fluorescence via hue to calculate Q_1 and weights the fluorescent region via its concentration c to compute the areal centroid for Q_3. The edges of fluorescent regions are detected via the Canny-algorithm.

2.2. Additional Measurements

The degree of relapse of carrier cavity is subjectively evaluated by independent visual inspection of three persons that are otherwise not involved in the research. The evaluators award points between zero (worst) and ten (best) according to a given exemplary chart. For each plate, the independently awarded points are averaged for the final quantification, Q_{ce}.

Distributions of fiber angles are measured in the concentric region of each plate with the Profactor fiber angle sensor. The quantifying parameter for the fiber angle distributions is the kurtosis k_t. Angles from the sewing threads are omitted from the measurements.

2.3. Design of Experiments and Materials

Two independent DoE plans for WCM and CIP in connection with the method of fluorescent photography build the base for the study. Analysis of fluorescent photography, subjective visual evaluation of elimination of carrier cavities and fiber angle measurements provide quantitative data of the dependent variables in the DoE.

In CIP, initial process evaluation led to the hypothesis that carrier cavity elimination might be linked to rearrangement of stretched polymer molecules under heat. To allow for a stable process, only the tool temperature T_t and the heating time inside the tool t_h are varied. All other parameters are held constant. A full factorial plan with a center point is selected for the DoE, Figure 3 A.

In case of WCM, the matrix is pre-applicated on the fiber material directly. Matrix temperature, determined by the temperature of the resin component T_r, and the pre-application time t_{pa} as well as press velocity of the tool v_p are relevant parameters. In case of non-linear correlations of t_r, three factor steps are structured in a quadratic DoE plan of a central-composite design [9, p. 37-39], Figure 3 B.

The DoE for CIP requires a carrier with a total of 109 cavities in shape of conical sections of 13 mm cross section. Each cavity can store 1.04 g of matrix each. The final carriers are stored at −18 °C until

Excerpt from ISBN 978-3-00-053387-7

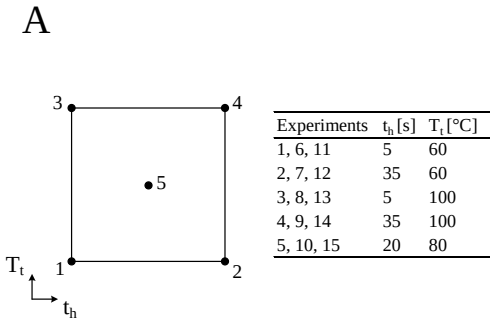

Experiments	t_h [s]	T_t [°C]
1, 6, 11	5	60
2, 7, 12	35	60
3, 8, 13	5	100
4, 9, 14	35	100
5, 10, 15	20	80

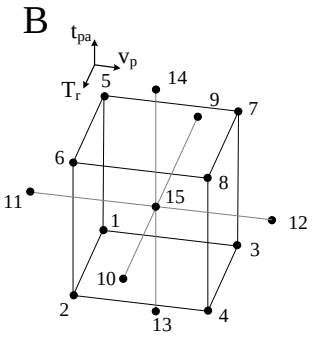

Experiments	T_r [°C]	v_p [mm/s]	t_{pa} [s]
1, 18, 35	35	3.5	5
2, 19, 36, 52*	54	3.5	5
3, 20, 37	35	9	5
4, 21, 38	54	9	5
5, 22, 39	35	3.5	15
6, 23, 40	54	3.5	15
7, 24, 41	35	9	15
8, 25, 42	54	9	15
9, 26, 43	27.11	6.25	10
10, 27, 44, 53*	61.89	6.25	10
11, 28, 45	44.5	1.22	10
12, 29, 46	44.5	11.29	10
13, 30, 47	44.5	6.25	0.85
14, 31, 48	44.5	6.25	19.15
15, 16, 17	44.5	6.25	10

Figure 3. Design of experiments for CIP (A) and WCM (B)

just before the respective press experiment. For WCM, a carrier without cavities is used.

Within the DoE, both processes, CIP and WCM are used to produce 2 mm thick composites plates with a diameter of 190 mm and a fiber volume content of 0.52. A circular stack of a diameter of 180 mm of CB300BX NCF (Hacotech) with ply sequence $[0°\ /90°,\ +/-\ 45°,\ +/-45°]_s$ is assembled manually from machine-cut plies using an angle template. The carrier film SV 250, either with cavities for CIP or without cavities for WCM, is fixed in stretched state with a clamping ring. The prepared fiber stack is concentrically placed on the carrier film first for WCM or subsequent to matrix pre-application for CIP. The matrix system resin XB3585 and hardener XB3458 (Huntsman) is used for all experiments. XB3585 is prepared in batches with 3 w-% internal release agent PAT-657/BW (Wuertz), either neat or marked with 0.25 w-% EpoDye in reference to the pure XB3585 mass. To prepare the matrix system for manual application, two paper cups are equipped with 50 g XB3585/PAT-657/BW and 20 g fluorescent XB3585/PAT-657/BW from the prepared batches, respectively. Both are heated to the temperature T_r of the respective experiment for WCM or to 40 °C in case of CIP. Two syringes are filled with 9.22 g and 3.67 g XB3458 for the neat and marked resin. Both hardener masses are injected simultaneously into the paper cups containing the pre-heated resin (time $t = 0$). Both compounds are mixed manually with wooden scoopulas for 15 s before manual pre-application on the NCF stack. A volume of 7 ml of fluorescent matrix is taken into a syringe and expelled on the NCF within the central ring of the dosing template for WCM or into the center carrier cavity for CIP. Simultaneously, the neat matrix is pre-applicated around the central ring or into all other carrier cavities directly from the cup. After insertion of the materials into the tool, the press is closed to to the holding/evacuation stage at 24.31 ± 0.63 mm with 5 mm/s. For CIP, the tool remains in this position for t_h prescribed by the DoE. In both processes the cavity is evacuated to under 10 mbar. The tool is then closed completely with $v_p = 5$ mm/s for CIP or with the prescribed speed in WCM. The curing cycle is set between 2.5 min and 25 min depending on the tool temperature in the respective experiment.

3. Results

The compactness of the fluorescent matrix distribution showed a strong dependency on the process parameters for both processes, WCM and CIP. Figure 4 depicts most and least compact distributions from digital images of plates after segmentation of the fluorescent phase.

For WCM, the distribution of fluorescent matrix was more compact and centered around its initial center position in experiment 41 than in experiment 23. The matrix in the latter is scattered chaotically over the lower half of the part. Q_1 only increases between top and bottom side of the part if distribution is compact (7, 24 and 41). If flow is scattered on top, matrix flow in z-direction is low.

Excerpt from ISBN 978-3-00-053387-7

For CIP, fluorescent matrix distribution is overall more compact compared to WCM. Fluorescent matrix on the bottom side of experiment 8 (D.2) is centered coherently around its initial pre-application region in the circular shape of the carrier cavity. On the top side of the same part (D.1), the fluorescent phase is slighty more scattered and larger. The centroid coordinates remained close to zero. At longer t_h but the same temperature (experiment 4), matrix distribution became more scattered

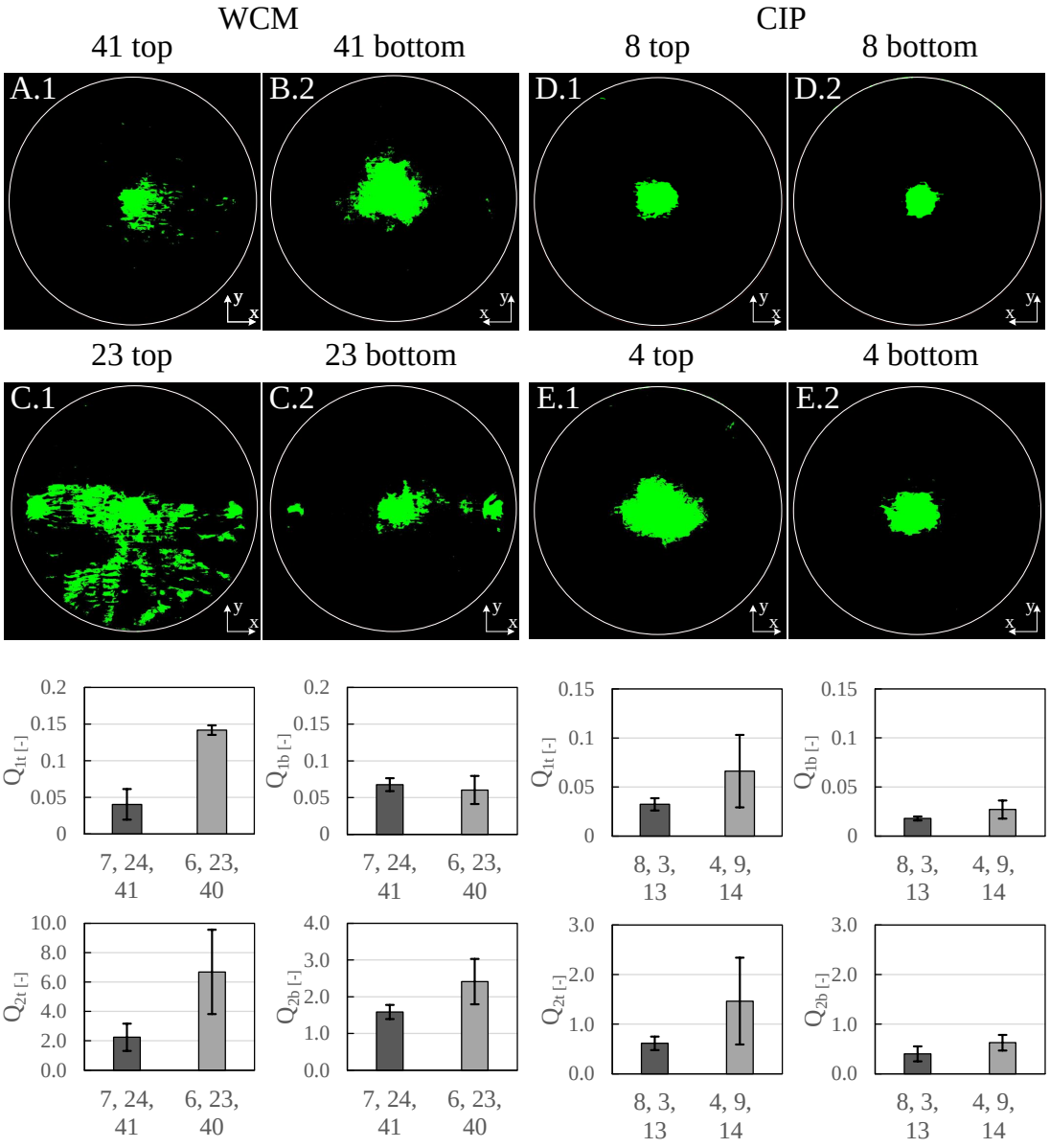

Figure 4. Most and least compact matrix distributions for WCM and CIP with standard deviation within plots

Results from all experiments were entered in Modde 10.1 to assess R^2, Q^2, model validity and reproducibility of each response. Responses were only deemed eligible for further analysis, if Q^2 was larger than 0.1 and validity was greater than 0.25. Effects of process parameters on eligible responses are depicted in two dimensional contour plots.

In case of WCM, since influence of t_{pa} on most responses was very weak, contour plots for T_r and v_p are shown for a constant t_{pa} of 10 s, Figure 5. Areal share of fluorescent phase Q_{1t}, its relative edge length Q_{2t} and the kurtosis of fiber angle distribution k_t improved when the resin temperature T_r was decreased

Excerpt from ISBN 978-3-00-053387-7

and the press speed v_p was increased. With increasing T_r and decreasing v_p, fluorescent matrix was increasingly scattered over the top side of the part. Fiber waviness showed the same correlation to the process parameters with the lowest waviness for low T_r of 35 °C and a high v_p of 9 mm/s.

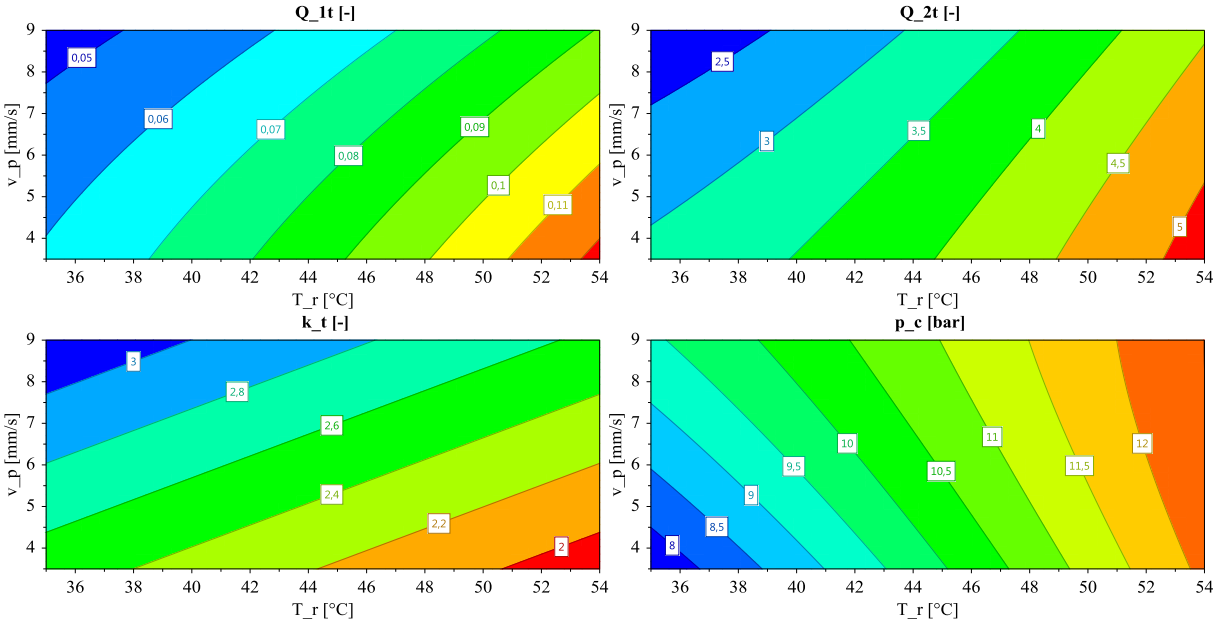

Figure 5. Effects of process parameters T_r and v_p on quality parameters Q_{1t}, Q_{2t}, k_t and p_c for WCM

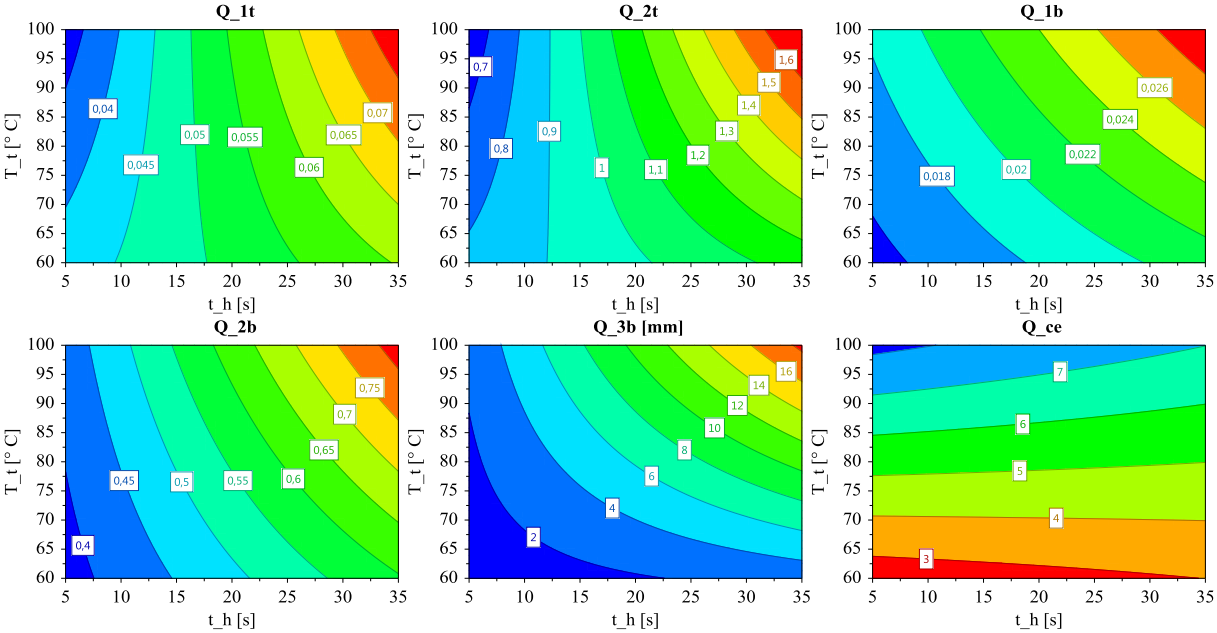

Figure 6. Effects of process parameters t_h and T_t on quality parameters Q_{1t}, Q_{2t}, Q_{1b}, Q_{2b}, Q_{3b} and Q_{ce} for CIP

In case of CIP, on the top side Q_{1t} and Q_{2t} showed consistent influences from the process parameters. In particular, the heating time t_h had a strong effect on the compactness of matrix distribution. It improved with low heating times t_h with an optimum at 5 s and 100 °C tool temperature. Similar results were exhibited from the bottom side. The bottom centroid shift of fluorescent phase $Q3b$ was influenced with the same principle effect as areal share and edge length. Thus, the lowest shift occurred in parts that were produced at t_h = 5 s and T_t = 60 °C and lengthened with increasing heating time and tool temperature.

Excerpt from ISBN 978-3-00-053387-7

4. Conclusion

Matrix distributions lend evidence to the hypothesis that matrix pre-application can lead to heterogenic flow in WCM. Matrix applied on top of the fiber stack forms a film, which is dislocated when the materials are transferred into the press and when the mold is closed. Both causes lateral flow an lower flow in through-thickness direction. At higher resin temperatures this dislocation is higher because matrix viscosity is lower. Later in the process however, these higher temperatures lead to a higher degree of cure. The higher viscosity of the matrix leads to higher cavity pressures and stronger fiber distortion.

In CIP, the cavities in which the applied matrix is stored, can restrict any lateral flow prior to insertion into the press. When the materials are located inside the press, matrix containment can be precisely controlled by heat flux into the film. The higher the temperature and the longer the film is exposed to the heat, the more cavities relapse and eject matrix prior to pressing. Generally, through-thickness flow dominates the impregnation in CIP as hypothesized in Figure 1.

Acknowledgments

The presented study was funded by the Bavarian Research Foundation under the grant AZ-1088-13 in cooperation with Toyota Boshoku, Dekumed Kunststoff und Maschinenvertrieb GmbH & Co. KG, Infiana and TUM Graduate School. The authors are grateful for the generous and faithful support.

References

[1] S. Bickerton and S. G. Advani. Characterizatrion and modeling of racetracking in liquid composite molding processes. *Composites Science and Technology*, 59:2215–2229, 1999.

[2] F. Dirschmid. Die cfk-karosserie des bmw i8 und deren auslegung. In G. Tecklenburg, editor, *Karosseriebautage Hamburg*, Proceedings, pages 217–231, Wiesbaden, 2014. Springer Fachmedien Wiesbaden.

[3] Erich Fries. Hochdruck-rtm technologie für die großserienproduktion von carbonfaserverstärkten kunststoffbauteilen. In *Materialica 2010*.

[4] Daniel Hofbauer, Lothar Kroll, Jörg Kaufmann, Andreas Repper, and Hanno Pfitzer. Faserverbundtechnologien für automobilkomponenten in der großserie. *Lightweight Design*, 7(6):40–45, 2014.

[5] D. Pradhan, A. K.and Das, R. Chattopahdyay, and S. N. Singh. Effect of 3d fiber orientation distribution on transverse air permeability of fibrous porous media. *Powder Technology*, 221:101–104, May 2012.

[6] P. Bockelmann, D. Haeffelin, and K. Drechsler. Method for producing a component from a fibre composite material, pressing blank therefor and component, May 2014.

[7] P. Bockelmann, D. Haeffelin, and K. Drechsler. Carrier-integrated pressing: An alternative impregnation process for automated processing of thermoset continuous fiber-reinforced laminates. pages 1–20, Apr 2015.

[8] B. Jaehne. *Digitale Bildverarbeitung*. Springer Vieweg, 7 edition, 2012.

[9] K. Siebertz, D. van Bebber, and T. Hochkirchen. *Design of Experiments (DoE)*. Springer Berlin Heidelberg, 1 edition, 2010.